
Dynamic Damage Propagation with Memory: A State-Based Model

Robert Lipton, Eyad Said, and Prashant K. Jha

Contents

Introduction	2
Formulation	3
Existence of Solutions	7
Energy Balance	14
Explicit Damage Models, Cyclic Loading, and Strain to Failure	18
Numerical Results	21
Periodic Loading	22
Shear Loading	23
Linear Elastic Operators in the Small Horizon Limit	25
Conclusions	27
References	28

Abstract

A model for dynamic damage propagation is developed using nonlocal potentials. The model is posed using a state-based peridynamic formulation. The resulting evolution is seen to be well posed. At each instant of the evolution, we identify a damage set. On this set, the local strain has exceeded critical values either for tensile or hydrostatic strain, and damage has occurred. The damage set is nondecreasing with time and is associated with damage state variables defined at each point in the body. We show that a rate form of energy balance holds at each time during the evolution. Away from the damage set, we show that the

R. Lipton (✉)

Department of Mathematics and Center for Computation and Technology, Louisiana State University, Baton Rouge, LA, USA

e-mail: lipton@lsu.edu

E. Said · P. K. Jha

Department of Mathematics, Louisiana State University, Baton Rouge, LA, USA

e-mail: esaid1@lsu.edu; prashant.j16o@gmail.com

nonlocal model converges to the linear elastic model in the limit of vanishing nonlocal interaction.

Keywords

Damage model · Nonlocal interactions · Energy dissipation · State-based peridynamics

Introduction

In this chapter, we address the problem of damage propagation in materials. Here the damage evolution is not known a priori and is found as part of the problem solution. Our approach is to use a nonlocal formulation with the purpose of using the least number of parameters to describe the model. We will work within the small deformation setting, and the model is developed within a state-based peridynamic formulation. Here strains are expressed in terms of displacement differences as opposed to spatial derivatives. For the problem at hand, the nonlocality provides the flexibility to simultaneously model non-differentiable displacements and damage evolution. The net force acting on a point x is due to the strain between x and neighboring points y . The neighborhood of nonlocal interaction between x and its neighbors y is confined to ball of radius δ centered at x denoted by $B_\delta(x)$. The radius of the ball is called the horizon. Numerical implementations based on nonlocal peridynamic models exhibit formation and localization of features associated with phase transformation and fracture (see, e.g., Dayal and Bhattacharya 2006; Silling and Lehoucq 2008; Silling et al. 2010; Foster et al. 2011; Agwai et al. 2011; Lipton et al. 2016; Bobaru and Hu 2012; Ha and Bobaru 2010; Silling and Bobaru 2005; Weckner and Abeyaratne 2005; Gerstle et al. 2007; Weckner and Emmrich 2005). A recent review can be found in Bobaru et al. (2016).

The recent model studied in Lipton (2014, 2016), Lipton et al. (2016), and Jha and Lipton (2017) is defined by double-well two-point strain potentials. Here one potential well is centered at the origin and associated with elastic response, while the other well is at infinity and associated with surface energy. The rationale for studying these models is that they are shown to be well posed, and in the limit of vanishing nonlocality, the dynamics recovers features associated with sharp fracture propagation (see Lipton 2014, 2016). While memory is not incorporated in this model, it is seen that the inertia of the evolution keeps the forces in a softened state over time as evidenced in simulations (Lipton et al., 2016). This modeling approach is promising for fast cracks, but for cyclic loading and slowly propagating fractures, an explicit damage-fracture modeling with memory is needed. In this work, we develop this approach for more general models that allow for three-point nonlocal interactions and irreversible damage. The use of three-point potentials allows one to model a larger variety of elastic properties. In the lexicon of peridynamics, we adopt an ordinary state-based formulation (Silling, 2000; Silling et al., 2007). We introduce nonlocal forces that soften irreversibly as the shear strain or dilatational strain increases beyond critical values. This model is shown

to deliver a mathematically well-posed evolution. Our proof of this is motivated by recent work Emrich and Phulst (2016) where existence of solution for bond-based peridynamic models with damage is established. Recently another well-posed bond-based model with damage has been proposed in Du et al. (2017) where fracture simulations are carried out.

In addition to being state based, our modeling approach differs from Emrich and Phulst (2016) and earlier bond-based work Silling and Askari (2005) and uses differentiable damage variables. This feature allows us to establish an energy balance equation relating kinetic energy, potential energy, and energy dissipation at each instant during the evolution. At each instant, we identify the set undergoing damage where the local energy dissipation rate is positive. On this set, the local strain has exceeded a critical value, and damage has occurred. Damage is irreversible, and the damage set is monotonically increasing with time. Explicit damage models are illustrated, and stress strain curves for both cyclic loading and strain to failure are provided. These models are illustrated in two numerical examples. In the first example, we consider a square domain and apply a time periodic y -directed displacement along the top edge while fixing the bottom, left and right edges. We track the strain and force over three loading periods. The simulations show that bonds suffer damage and the strain vs force plot is similar to the one predicted by the damage law (see Fig. 14). In the second example, we apply a shear load to the top edge while fixing the bottom edge and leaving left and right edges free. As expected, we find that damage appears along the diagonal of square (see Fig. 15).

We conclude by noting that for this model the forces scale inversely with the length of the horizon. With this in mind, we consider undamaged regions, and we are able to show that the nonlocal operator converges to a linear local operator associated with the elastic wave equation. In this limit, the elastic tensor can have any combination of Poisson's ratio and Young's modulus. The Poisson's ratio and Young modulus are determined uniquely by explicit formulas in terms of the nonlocal potentials used to define the model. This result is consistent with small horizon convergence results for convex energies (see Emrich and Weckner 2007; Mengesha and Du 2014; Silling and Lehoucq 2008). Further reading and complete derivations can be found in the recent monograph Lipton et al. (2018).

Formulation

In this work, we assume the displacements u are small (infinitesimal) relative to the size of the three-dimensional body D . The tensile strain is denoted $S = S(y, x, t; u)$ and given by

$$S(y, x, t; u) = \frac{u(t, y) - u(t, x)}{|y - x|} \cdot e_{y-x}, \quad e_{y-x} = \frac{y - x}{|y - x|}, \quad (1)$$

where e_{y-x} is a unit direction vector and \cdot is the dot product. It is evident that $S(y, x, t; u)$ is the tensile strain along the direction e_{y-x} . We introduce the nonnegative weight $\omega^\delta(|y-x|)$ such that $\omega^\delta = 0$ for $|y-x| > \delta$ and the hydrostatic strain at x is defined by

$$\theta(x, t; u) = \frac{1}{V_\delta} \int_{D \cap B_\delta(x)} \omega^\delta(|y-x|) |y-x| S(y, x, t; u) dy, \quad (2)$$

where V_δ is the volume of the ball $B_\delta(x)$ of radius δ centered at x . The weight is chosen such that $\omega^\delta(|y-x|) = \omega(|y-x|/\delta)$ and

$$\ell_1 = \frac{1}{V_\delta} \int_{B_\delta(x)} \omega^\delta(|y-x|) dy < \infty. \quad (3)$$

We follow Silling (2000) and Emrich and Phulst (2016) and introduce a nonnegative damage factor taking the value one in the undamaged region and zero in the fully damaged region. The damage factor for the force associated with tensile strains is written $H^T(u)(y, x, t)$; the corresponding factor for hydrostatic strains is written $H^D(u)(x, t)$. Here we assume no damage and $H^T(u)(y, x, t) = 1$ until a critical tensile strain S_c is reached. For tensile strains greater than S_c , damage is initiated and $H^T(y, x, t)$ drops below 1. The fully damaged state is $H^T(y, x, t) = 0$. For hydrostatic strains, we assume no damage until a critical positive dilatational strain θ_c^+ or a negative compressive strain (θ_c^-) is reached. Again $H^D(x, t) = 1$ until a critical hydrostatic strain is reached and then drops below 1 with the fully damaged state being $H^D(x, t) = 0$. We postpone description of the specific form of the history-dependent damage factors until after we have defined the nonlocal forces.

The force at a point x due to tensile strain is given by

$$\begin{aligned} \mathcal{L}^T(u)(x, t) &= \frac{2}{V_\delta} \int_{D \cap B_\delta(x)} \frac{J^\delta(|y-x|)}{\delta|y-x|} H^T(u)(y, x, t) \partial_S \\ &f(\sqrt{|y-x|} S(y, x, t; u)) e_{y-x} dy, \end{aligned} \quad (4)$$

Here $J^\delta(|y-x|)$ is a nonnegative bounded function such that $J^\delta = 0$ for $|y-x| > \delta$ and $M = \sup\{y \in B_\delta(x); J^\delta(|y-x|)\}$ and

$$\ell_2 = \frac{1}{V_\delta} \int_{B_\delta(x)} \frac{J^\delta(|y-x|)}{|y-x|^2} dy < \infty \text{ and } \ell_3 = \frac{1}{V_\delta} \int_{B_\delta(x)} \frac{J^\delta(|y-x|)}{|y-x|^{3/2}} dy < \infty. \quad (5)$$

Both J^δ and ω^δ are prescribed and characterize the influence of nonlocal forces on x by neighboring points y . Here ∂_S is the partial derivative with respect to strain. The function $f = f(r)$ is twice differentiable for all arguments r on the real line, and f' and f'' are bounded. Here we take $f(r) = \alpha r^2/2$ for $r < r_1$ and $f = r$ for

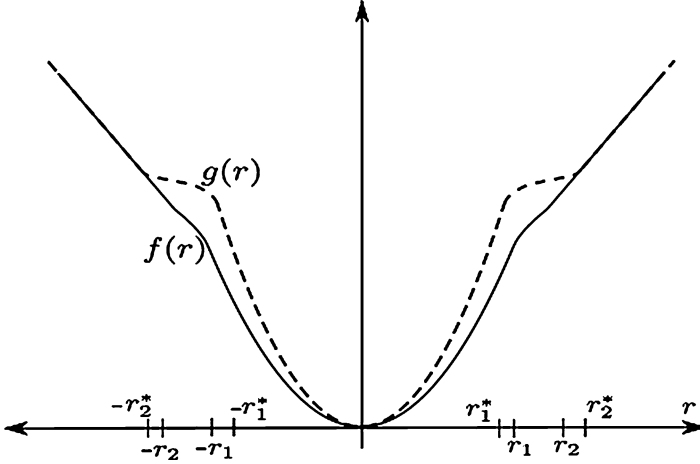


Fig. 1 Generic plot of $f(r)$ (Solid line) and $g(r)$ (Dashed line)

$r_2 < r$, with $r_1 < r_2$ (see Fig. 1). The factor $\sqrt{|y-x|}$ appearing in the argument of $\partial_S f$ ensures that the nonlocal operator \mathcal{L}^T converges to the divergence of a stress tensor in the small horizon limit when it's known a priori that displacements are smooth (see section “[Linear Elastic Operators in the Small Horizon Limit](#)”).

The force at a point x due to the hydrostatic strain is given by

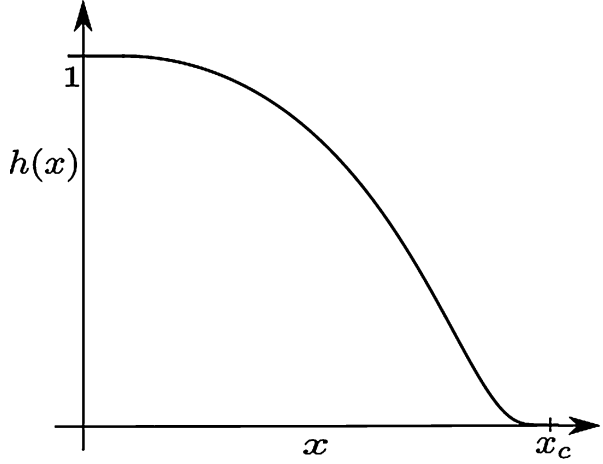
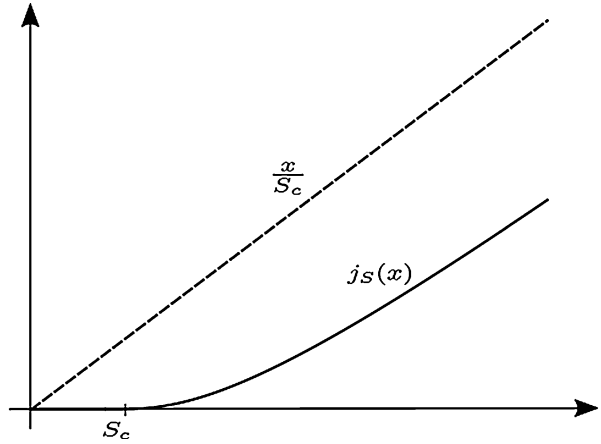
$$\mathcal{L}^D(u)(x, t) = \frac{1}{V_\delta} \int_{D \cap B_\delta(x)} \frac{\omega^\delta(|y-x|)}{\delta^2} [H^D(u)(y, t) \partial_\theta g(\theta(y, t; u)) + \quad (6)$$

$$H^D(u)(x, t) \partial_\theta g(\theta(x, t; u))] e_{y-x} dy, \quad (7)$$

where the function $g(r) = \beta r^2/2$ for $r < r_1^*$, $g = r$ for $r_2^* < r$, with $r_1^* < r_2^*$ and g is twice differentiable and g' and g'' are bounded (see Fig. 1). It is readily verified that the force $\mathcal{L}^T(u)(x, t) + \mathcal{L}^D(u)(x, t)$ satisfies balance of linear and angular momentum.

The damage factor for tensile strain $H^T(u)(y, x, t)$ is given in terms of the functions $h(x)$ and $j_S(x)$. Here h is nonnegative, has bounded derivatives (hence Lipschitz continuous), takes the value one for negative x and for $x \geq 0$ decreases, and is zero for $x > x_c$ (see Fig. 2). Here we are free to choose x_c to be any small and positive number. The function $j_S(x)$ is nonnegative, has bounded derivatives (hence Lipschitz continuous), takes the value zero up to a positive critical strain S_C , and then takes on positive values. We will suppose $j_S(x) \leq \gamma|x|$ for some $\gamma > 0$ (see Fig. 3). The damage factor is now defined to be

$$H^T(u)(y, x, t) = h \left(\int_0^t j_S(S(y, x, \tau; u)) d\tau \right). \quad (8)$$

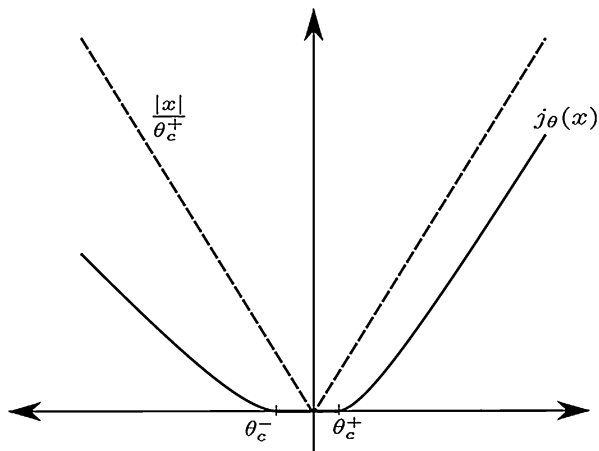
Fig. 2 Generic plot of $h(x)$ **Fig. 3** Generic plot of $j_S(x)$ with S_c 

It is clear from this definition that damage occurs when the stress exceeds S_c for some period of time and the bond force decreases irrevocably from its undamaged value. The damage function defined here is symmetric, i.e., $H^T(u)(y, x, t) = H^T(u)(x, y, t)$. For hydrostatic strain, we introduce the nonnegative function j_θ with bounded derivatives (hence Lipschitz continuous). We suppose $j_\theta = 0$ for an interval containing the origin given by (θ_c^-, θ_c^+) and take positive values outside this interval (see Fig. 4). As before we will suppose $j_\theta(x) \leq \gamma|x|$ for some $\gamma > 0$. The damage factor for hydrostatic strain is given by

$$H^D(u)(x, t) = h \left(\int_0^t j_\theta(\theta(x, \tau; u)) d\tau \right). \quad (9)$$

For this model, it is clear that damage can occur irreversibly for compressive or dilatational strain when the possibly different critical values θ_c^- or θ_c^+ are exceeded.

Fig. 4 Generic plot of $j_\theta(x)$ with θ_c^+ , and θ_c^-



The *damage set* at time t is defined to be the collection of all points x for which $H^T(y, x, t)$ or $H^D(u)(x, t)$ is less than one. This set is monotonically increasing in time. The *process zone* at time t is the collection of points x undergoing damage such that $\partial_t H^T(y, x, t) < 0$ or $\partial_t H^D(x, t) < 0$. Explicit examples of $H^T(u)(y, x, t)$ and $H^D(u)(x, t)$ are given in section “[Explicit Damage Models, Cyclic Loading, and Strain to Failure](#)”.

We define the body force $b(x, t)$, and the displacement $u(x, t)$ is the solution of the initial value problem given by

$$\rho \partial_t^2 u(x, t) = \mathcal{L}^T(u)(x, t) + \mathcal{L}^D(u)(x, t) + b(x, t) \text{ for } x \in D \text{ and } t \in (0, T), \quad (10)$$

with initial data

$$u(x, 0) = u_0(x), \quad \partial_t u(x, 0) = v_0(x). \quad (11)$$

It is easily verified that this is an ordinary state-based peridynamic model. We show in the next section that this initial value problem is well posed.

Existence of Solutions

The regularity and existence of the solution depend on the regularity of the initial data and body force. In this work, we choose a general class of body forces and initial conditions. The initial displacement u_0 and velocity v_0 are chosen to be integrable and bounded and belonging to $L^\infty(D; \mathbb{R}^3)$. The space of such functions is denoted by $L^\infty(D; \mathbb{R}^3)$. The body force $b(x, t)$ is chosen such that for every $t \in [0, T_0]$, b takes values in $L^\infty(D, \mathbb{R}^3)$ and is continuous in time. The associated norm is defined to be $\|b\|_{C([0, T_0]; L^\infty(D, \mathbb{R}^3))} = \max_{x \in [0, T_0]} \|b(x, t)\|_{L^\infty(D, \mathbb{R}^3)}$. The

associated space of continuous functions in time taking values in $L^\infty(D; \mathbb{R}^3)$ for which this norm is finite is denoted by $C([0, T_0]; L^\infty(D, \mathbb{R}^3))$. The space of functions twice differentiable in time taking values in $L^\infty(D, \mathbb{R}^3)$ such that both derivatives belong to $C([0, T_0]; L^\infty(D, \mathbb{R}^3))$ is written as $C^2([0, T_0]; L^\infty(D, \mathbb{R}^3))$. We now assert the existence and uniqueness for the solution of the initial value problem.

Theorem 1 (Existence and uniqueness of the damage evolution). *The initial value problem given by (10) and (11) has a solution $u(x, t)$ such that for every $t \in [0, T_0]$, u takes values in $L^\infty(D, \mathbb{R}^3)$ and is the unique solution belonging to the space $C^2([0, T_0]; L^\infty(D, \mathbb{R}^3))$.*

To prove the theorem, we will show

- (1) The operator $\mathcal{L}^T(u)(x, t) + \mathcal{L}^D(u)(x, t)$ is a map from $C([0, T_0]; L^\infty(D, \mathbb{R}^3))$ into itself.
- (2) The operator $\mathcal{L}^T(u)(x, t) + \mathcal{L}^D(u)(x, t)$ is Lipschitz continuous with respect to the norm of $C([0, T_0]; L^\infty(D, \mathbb{R}^3))$.

The theorem then follows from an application of the Banach fixed point theorem.

To establish properties (1) and (2), we state and prove the following lemmas for the damage factors.

Lemma 1. *Let $H^T(u)(y, x, t)$ and $H^D(u)(x, t)$ be defined as in (8) and (9). Then for $u \in C([0, T_0]; L^\infty(D, \mathbb{R}^3))$, the mappings*

$$(y, x) \mapsto H^T(u)(y, x, t) : D \times D \rightarrow \mathbb{R}, \quad x \mapsto H^D(u)(x, t) : D \rightarrow \mathbb{R} \quad (12)$$

are measurable for every $t \in [0, T_0]$, and the mappings

$$t \mapsto H^T(u)(y, x, t) : [0, T_0] \rightarrow \mathbb{R}, \quad t \mapsto H^D(u)(x, t) : [0, T_0] \rightarrow \mathbb{R} \quad (13)$$

are continuous for almost all (y, x) and x , respectively. Moreover for almost all $(y, x) \in D \times D$ and all $t \in [0, T_0]$, the map

$$u \mapsto H^T(u)(y, x, t) : C([0, T_0]; L^\infty(D, \mathbb{R}^3)) \rightarrow \mathbb{R} \quad (14)$$

is Lipschitz continuous, and for almost all $x \in D$ and all $t \in [0, T_0]$, the map

$$u \mapsto H^D(u)(x, t) : C([0, T_0]; L^\infty(D, \mathbb{R}^3)) \rightarrow \mathbb{R} \quad (15)$$

is Lipschitz continuous.

Proof. The measurability properties are immediate. In what follows, constants are generic and apply to the context in which they are used. We establish continuity in time for $H^D(u)$. For \hat{t} and t in $[0, T_0]$, we have

$$\begin{aligned}
& |H^D(u)(x, \hat{t}) - H^D(u)(x, t)| \\
&= \left| h \left(\int_0^{\hat{t}} j_\theta(\theta(x, \tau; u)) d\tau \right) - h \left(\int_0^t j_\theta(\theta(x, \tau; u)) d\tau \right) \right| \\
&\leq C_1 \int_{\min\{\hat{t}, t\}}^{\max\{\hat{t}, t\}} j_\theta(\theta(x, \tau; u)) d\tau \\
&\leq \gamma C_1 \int_{\min\{\hat{t}, t\}}^{\max\{\hat{t}, t\}} |\theta(x, \tau; u)| d\tau \\
&\leq \gamma \ell_1 C_1 C_2 |\hat{t} - t| 2 \|u\|_{C([0, T_0]; L^\infty(D, \mathbb{R}^3))}.
\end{aligned} \tag{16}$$

The first inequality follows from the Lipschitz continuity of h , the second follows from the growth condition on j_θ , and the third follows from (3).

We establish continuity in time for $H^T(u)$. For \hat{t} and t in $[0, T_0]$, we have

$$\begin{aligned}
& |H^T(u)(x, \hat{t}) - H^T(u)(x, t)| \\
&= \left| h \left(\int_0^{\hat{t}} j_S(S(y, x, \tau; u)) d\tau \right) - h \left(\int_0^t j_S(S(y, x, \tau; u)) d\tau \right) \right| \\
&\leq C_1 \int_{\min\{\hat{t}, t\}}^{\max\{\hat{t}, t\}} j_S(S(y, x, \tau; u)) d\tau \\
&\leq \gamma C_1 \int_{\min\{\hat{t}, t\}}^{\max\{\hat{t}, t\}} |S(y, x, \tau; u)| d\tau \\
&\leq \gamma C_1 C_2 \frac{|\hat{t} - t|}{|y - x|} 2 \|u\|_{C([0, T_0]; L^\infty(D, \mathbb{R}^3))}.
\end{aligned} \tag{17}$$

The first inequality follows from the Lipschitz continuity of h , the second follows from the growth condition on j_S , and the third follows from the definition of strain (1).

To demonstrate Lipschitz continuity for $H^D(u)(x, t)$, we write

$$\begin{aligned}
& |H^D(u)(x, t) - H^D(v)(x, t)| \\
&= \left| h \left(\int_0^t j_\theta(\theta(x, \tau; u)) d\tau \right) - h \left(\int_0^t j_\theta(\theta(x, \tau; v)) d\tau \right) \right| \\
&\leq C_1 \left| \int_0^t (j_\theta(\theta(x, \tau; u)) - j_\theta(\theta(x, \tau; v))) d\tau \right| \\
&\leq C_1 C_2 \int_0^t |\theta(x, \tau; u) - \theta(x, \tau; v)| d\tau \\
&\leq 2t \ell_1 C_1 C_2 \|u - v\|_{C([0, t]; L^\infty(D, \mathbb{R}^3))}.
\end{aligned} \tag{18}$$

The first inequality follows from the Lipschitz continuity of h , the second follows from the Lipschitz continuity of j_θ , and the third follows from (3). The Lipschitz continuity for $H^S(u)(y, x, t)$ follows from similar arguments using the Lipschitz continuity of h , j_S , and (1), and we get

$$\begin{aligned} & |H^T(u)(y, x, t) - H^T(v)(y, x, t)| \\ & \leq \frac{2tC_1C_2C_3}{|y-x|} \|u - v\|_{C([0,t];L^\infty(D,\mathbb{R}^3))}. \end{aligned} \quad (19)$$

□

Proof of Theorem 1. We establish (1) by first noting that

$$|\mathcal{L}^T(u)(x, t) + \mathcal{L}^D(u)(x, t)| \leq \frac{C}{\delta^2}, \quad (20)$$

where C is a constant. This estimate follows from the boundedness of f' , g' , $H^T(u)$, and $H^D(u)$ and the integrability of the ratios $J^\delta(|y-x|)/|y-x|^2$, $J^\delta(|y-x|)/|y-x|^{3/2}$, and $\omega^\delta(|y-x|)$. Thus $\|\mathcal{L}^T(u)(x, t) + \mathcal{L}^D(u)(x, t)\|_{L^\infty(D,\mathbb{R}^3)}$ is uniformly bounded for all $t \in [0, T_0]$.

To complete the demonstration of (1), we point out that the force functions $\partial_S f$ and $\partial_\theta g$ are Lipschitz continuous in their arguments. The key features are given in the following lemma.

Lemma 2. *Given two functions v and w in $L^\infty(D, \mathbb{R}^3)$, then*

$$\begin{aligned} & |\partial_S f(\sqrt{|y-x|}S(y, x; v)) - \partial_S f(\sqrt{|y-x|}S(y, x; w))| \\ & \leq \frac{2C}{\sqrt{|y-x|}} \|v - w\|_{L^\infty(D,\mathbb{R}^3)}. \end{aligned} \quad (21)$$

and

$$|\partial_\theta g(\theta(x; v)) - \partial_\theta g(\theta(x; w))| \leq 2\ell_1 C \|v - w\|_{L^\infty(D,\mathbb{R}^3)}. \quad (22)$$

Proof.

$$\begin{aligned} & |\partial_S f(\sqrt{|y-x|}S(y, x; v)) - \partial_S f(\sqrt{|y-x|}S(y, x; w))| \\ & \leq C \sqrt{|y-x|} |S(y, x; v) - S(y, x; w)| \leq \frac{2C}{\sqrt{|y-x|}} \|v - w\|_{L^\infty(D,\mathbb{R}^3)}, \end{aligned} \quad (23)$$

where the first inequality follows from the Lipschitz continuity of $\partial_S f$ and the second follows from the definition of S .

For $\partial_\theta g$, we have

$$|\partial_\theta g(\theta(x; v)) - \partial_\theta g(\theta(x; w))| \leq C|\theta(x; v) - \theta(x; w)| \leq 2\ell_1 C_1 \|v - w\|_{L^\infty(D, \mathbb{R}^3)}, \quad (24)$$

where the first inequality follows from the Lipschitz continuity of $\partial_\theta g$ and the second follows from the definitions of θ and S . \square

We have

$$\begin{aligned} & |\mathcal{L}^T(u)(x, \hat{t}) - \mathcal{L}^T(u)(x, t)| \\ & \leq \frac{2}{V_\delta} \int_{D \cap B_\delta(x)} \frac{J^\delta(|y-x|)}{\delta|y-x|} |\partial_S f(\sqrt{y-x} S(y, x, \hat{t}; u)) \\ & \quad - \partial_S f(\sqrt{y-x} S(y, x, t; u))| dy \\ & \quad + \frac{2}{V_\delta} \int_{D \cap B_\delta(x)} \frac{J^\delta(|y-x|)}{\delta|y-x|} |H^T(u)(y, x, \hat{t}) - H^T(u)(y, x, t)| dy. \end{aligned} \quad (25)$$

From the above, (19), and Lemma 2, we see that

$$\begin{aligned} & \|\mathcal{L}^T(u)(x, \hat{t}) - \mathcal{L}^T(u)(x, t)\|_{L^\infty(D, \mathbb{R}^3)} \\ & \leq \frac{\ell_3 C_3}{\delta} \|u(x, \hat{t}) - u(x, t)\|_{L^\infty(D, \mathbb{R}^3)} + \frac{\ell_2 \gamma C_1 C_2}{\delta} |\hat{t} - t| 2 \|u\|_{C([0, T_0]; L^\infty(D, \mathbb{R}^3))} \end{aligned} \quad (26)$$

and we see \mathcal{L}^T is well defined and maps $C([0, T_0]; L^\infty(D, \mathbb{R}^3))$ into itself.

We show the continuity in time for $\mathcal{L}^D(u)(x, t)$. Now we have

$$\begin{aligned} & |\mathcal{L}^D(u)(x, \hat{t}) - \mathcal{L}^D(u)(x, t)| \\ & \leq \frac{1}{V_\delta} \int_{D \cap B_\delta(x)} \frac{\omega^\delta(|y-x|)}{\delta^2} |\partial_\theta g(\theta(y, \hat{t}; u)) - \partial_\theta g(\theta(y, t; u))| dy \\ & \quad + \frac{1}{V_\delta} \int_{D \cap B_\delta(x)} \frac{\omega^\delta(|y-x|)}{\delta^2} |H^D(u)(y, \hat{t}) - H^D(u)(y, t)| dy \\ & \quad + \frac{1}{V_\delta} \int_{D \cap B_\delta(x)} \frac{\omega^\delta(|y-x|)}{\delta^2} |\partial_\theta g(\theta(x, \hat{t}; u)) - \partial_\theta g(\theta(x, t; u))| dy \\ & \quad + \frac{1}{V_\delta} \int_{D \cap B_\delta(x)} \frac{\omega^\delta(|y-x|)}{\delta^2} |H^D(u)(x, \hat{t}) - H^D(u)(x, t)| dy \end{aligned} \quad (27)$$

and applying Lemma 2 and (18)–(27), we get the continuity

$$\begin{aligned} & |\mathcal{L}^D(u)(x, \hat{t}) - \mathcal{L}^D(u)(x, t)| \leq \frac{4\ell_1^2 C_1}{\delta^2} \|u(\hat{t}, x) - u(t, x)\|_{L^\infty(D, \mathbb{R}^3)} \\ & \quad + \frac{\gamma 4\ell_1^2 C_1 C_2}{\delta^2} |\hat{t} - t| \|u\|_{C([0, T_0]; L^\infty(D, \mathbb{R}^3))}. \end{aligned} \quad (28)$$

We conclude that \mathcal{L}^D is well defined and maps $C([0, T_0]; L^\infty(D, \mathbb{R}^3))$ into itself and item (1) is proved.

To show Lipschitz continuity, consider any two functions u and w belonging to $C([0, T_0]; L^\infty(D, \mathbb{R}^3))$, $t \in [0, T_0]$ to write

$$\begin{aligned}
& |\mathcal{L}^T(u)(x, t) + \mathcal{L}^D(u)(x, t) - [\mathcal{L}^T(w)(x, t) + \mathcal{L}^D(w)(x, t)]| \\
& \leq \frac{2}{V_\delta} \int_{D \cap B_\delta(x)} \frac{J^\delta(|y-x|)}{\delta|y-x|} |\partial_S f(\sqrt{|y-x|} S(y, x, t; u)) \\
& \quad - \partial_S f(\sqrt{|y-x|} S(y, x, t; w))| dy \\
& \quad + \frac{2}{V_\delta} \int_{D \cap B_\delta(x)} \frac{J^\delta(|y-x|)}{\delta|y-x|} |H^T(u)(y, x, t) - H^T(w)(y, x, t)| dy \\
& \quad + \frac{1}{V_\delta} \int_{D \cap B_\delta(x)} \frac{\omega^\delta(|y-x|)}{\delta^2} |\partial_\theta g(\theta(y, t; u)) - \partial_\theta g(\theta(y, t; w))| dy \\
& \quad + \frac{1}{V_\delta} \int_{D \cap B_\delta(x)} \frac{\omega^\delta(|y-x|)}{\delta^2} |H^D(u)(y, t) - H^D(w)(y, t)| dy \\
& \quad + \frac{1}{V_\delta} \int_{D \cap B_\delta(x)} \frac{\omega^\delta(|y-x|)}{\delta^2} |\partial_\theta g(\theta(x, t; u)) - \partial_\theta g(\theta(x, t; w))| dy \\
& \quad + \frac{1}{V_\delta} \int_{D \cap B_\delta(x)} \frac{\omega^\delta(|y-x|)}{\delta^2} |H^D(u)(x, t) - H^D(w)(x, t)| dy.
\end{aligned} \tag{29}$$

Applying (18) and (19)–(29) delivers the estimate

$$\begin{aligned}
& \|\mathcal{L}^T(u)(x, t) + \mathcal{L}^D(u)(x, t) - [\mathcal{L}^T(w)(x, t) + \mathcal{L}^D(w)(x, t)]\|_{C([0, t]; L^\infty(D, \mathbb{R}^3))} \\
& \leq \frac{C_1 + tC_2}{\delta^2} \|u - w\|_{C([0, t]; L^\infty(D, \mathbb{R}^3))},
\end{aligned} \tag{30}$$

where C_1 and C_2 are constants not depending on time u or w . For $T_0 > t$, we can choose a constant $L > (C_1 + T_0 C_2)/\delta^2$ and

$$\begin{aligned}
& \|\mathcal{L}^T(u)(x, t) + \mathcal{L}^D(u)(x, t) - [\mathcal{L}^T(w)(x, t) + \mathcal{L}^D(w)(x, t)]\|_{C([0, t]; L^\infty(D, \mathbb{R}^3))} \\
& \leq L \|u - w\|_{C([0, t]; L^\infty(D, \mathbb{R}^3))}, \text{ for all } t \in [0, T_0].
\end{aligned} \tag{31}$$

This proves the Lipschitz continuity, and item (2) of the theorem is proved. Note that $u(\tau) = w(\tau)$ for all $\tau \in [0, t]$ implies $\mathcal{L}^T(u)(x, t) + \mathcal{L}^D(u)(x, t) = [\mathcal{L}^T(w)(x, t) + \mathcal{L}^D(w)(x, t)]$ and $\mathcal{L}^T(u)(x, t) + \mathcal{L}^D(u)(x, t)$ is a Volterra operator.

We write evolutions $u(x, t)$ belonging to $C([0, t]; L^\infty(D, \mathbb{R}^3))$ as $u(t)$ and $(Vu)(t)$ is the sum

$$(Vu)(t) = \mathcal{L}^T(u)(t) + \mathcal{L}^D(u)(t). \quad (32)$$

We seek the unique fixed point of $u(t) = (Iu)(t)$ where I maps $C([0, t]; L^\infty(D, \mathbb{R}^3))$ into itself and is defined by

$$(Iu)(t) = u_0 + tv_0 + \int_0^t (t - \tau)(Vu)(\tau) + b(\tau) d\tau. \quad (33)$$

This problem is equivalent to finding the unique solution of the initial value problem given by (10) and (11). We now show that I is a contraction map, and by virtue of the Banach fixed point theorem, we can assert the existence of a fixed point in $C([0, t]; L^\infty(D, \mathbb{R}^3))$. To see that I is a contraction map on $C([0, t]; L^\infty(D, \mathbb{R}^3))$, we introduce the equivalent norm

$$\| \|u\| \|_{C([0, t]; L^\infty(D, \mathbb{R}^3))} = \max_{t \in [0, T_0]} \{e^{-2LT_0 t} \|u\|_{L^\infty(D, \mathbb{R}^3)}\}, \quad (34)$$

and show I is a contraction map with respect to this norm. We apply (30) to find for $t \in [0, T_0]$ that

$$\begin{aligned} \|(Iu)(t) - (Iw)(t)\|_{L^\infty(D, \mathbb{R}^3)} &\leq \int_0^t (t - \tau) \|(Vu)(\tau) - (Vw)(\tau)\|_{L^\infty(D, \mathbb{R}^3)} d\tau \\ &\leq LT_0 \int_0^t \|u - w\|_{C([0, \tau]; L^\infty(D, \mathbb{R}^3))} d\tau \\ &\leq LT_0 \int_0^t \max_{s \in [0, \tau]} \{ \|u(s) - w(s)\|_{L^\infty(D, \mathbb{R}^3)} e^{-2LT_0 s} \} e^{2LT_0 \tau} d\tau \\ &\leq \frac{e^{2LT_0 t} - 1}{2} \| \|u - w\| \|_{C([0, T_0]; L^\infty(D, \mathbb{R}^3))}, \end{aligned} \quad (35)$$

and we conclude

$$\| \| (Iu)(t) - (Iw)(t) \| \|_{C([0, T_0]; L^\infty(D, \mathbb{R}^3))} \leq \frac{1}{2} \| \|u - w\| \|_{C([0, T_0]; L^\infty(D, \mathbb{R}^3))}, \quad (36)$$

so I is a contraction map. From the Banach fixed point theorem, there is a unique fixed point $u(t)$ belonging to $C([0, T_0]; L^\infty(D, \mathbb{R}^3))$, and it is evident from (33) that $u(t)$ also belongs to $C^2([0, T_0]; L^\infty(D, \mathbb{R}^3))$. This concludes the proof of Theorem 1.

Energy Balance

The evolution is shown to exhibit a balance of energy at all times. In this section, we describe the potential and the energy dissipation rate and show energy balance in rate form. The potential energy at time t for the evolution is denoted by $U(t)$ and is given by

$$U(t) = \frac{2}{V_\delta} \int_D \int_{D \cap B_\delta(x)} \frac{J^\delta(|y-x|)}{\delta} H^T(u)(y, x, t) f(\sqrt{|y-x|} S(y, x, t; u)) dy dx + \int_D \frac{1}{\delta^2} H^D(u)(x, t) g(\theta(x, t; u)) dx. \quad (37)$$

The energy dissipation rate $\partial_t R(t)$ is

$$\partial_t R(t) = -\frac{2}{V_\delta} \int_D \int_{D \cap B_\delta(x)} \frac{J^\delta(|y-x|)}{\delta} \partial_t H^T(u)(y, x, t) f(\sqrt{|y-x|} S(y, x, t; u)) dy dx - \int_D \frac{1}{\delta^2} \partial_t H^D(u)(x, t) g(\theta(x, t; u)) dx. \quad (38)$$

The derivatives $\partial_t H^T(u)(y, x, t)$ and $\partial_t H^D(u)(x, t)$ are easily seen to be nonpositive, and the dissipation rate satisfies $\partial_t R(t) \geq 0$. The kinetic energy is

$$K(t) = \rho \int_D \frac{|\partial_t u(x, t)|^2}{2} dx. \quad (39)$$

The energy balance in rate form is given in the following theorem.

Theorem 2. *The rate form of energy balance for the damage-fracture evolution is given by*

$$\partial_t K(t) + \partial_t U(t) + \partial_t R(t) = \int_D b(x, t) \cdot \partial_t u(x, t) dx. \quad (40)$$

Proof of Theorem 2. We multiply both sides of the evolution Eq. (10) by $\partial_t u(x, t)$ and integrate over D to get

$$\rho \int_D \partial_t^2 u(x, t) \cdot \partial_t u(x, t) dx = \int_D \mathcal{L}^T(u)(x, t) \cdot \partial_t u(x, t) dx \quad (41)$$

$$+ \int_D \mathcal{L}^D(u)(x, t) \cdot \partial_t u(x, t) dx + \int_D b(x, t) \cdot \partial_t u(x, t) dx. \quad (42)$$

The term on the left side of the equation is immediately recognized as $\partial_t K(t)$. The first and second terms on the right-hand side of the equation are given in the following lemma.

Lemma 3. *One has the following integration by parts formulas given by*

$$\begin{aligned} & \int_D \mathcal{L}^T(u)(x, t) \cdot \partial_t u(x, t) dx \\ &= -\frac{2}{V_\delta} \int_D \int_{D \cap B_\delta(x)} \frac{J^\delta(|y-x|)}{\delta} H^T(u)(y, x, t) \partial_t f(\sqrt{|y-x|} S(y, x, t; u)) dy dx. \end{aligned} \quad (43)$$

and

$$\int_D \mathcal{L}^D(u)(x, t) \cdot \partial_t u(x, t) dx = - \int_D \frac{1}{\delta^2} H^D(u)(x, t) \partial_t g(\theta(x, t; u)) dx. \quad (44)$$

Now note that

$$\begin{aligned} & \partial_t U(t) + \partial_t R(t) \\ &= \frac{2}{V_\delta} \int_D \int_{D \cap B_\delta(x)} \frac{J^\delta(|y-x|)}{\delta} H^T(u)(y, x, t) \partial_t f(\sqrt{|y-x|} S(y, x, t; u)) dy dx \\ &+ \int_D \frac{1}{\delta^2} H^D(u)(x, t) \partial_t g(\theta(x, t; u)) dx, \end{aligned} \quad (45)$$

and the energy balance theorem follows from (41) and (45).

We conclude by proving the integration by parts Lemma 3. We start by proving (44). We expand $\partial_t g(\theta(x, t))$

$$\begin{aligned} & \partial_t g(\theta(x, t; u)) \\ &= \partial_\theta g(\theta(x, t; u)) \frac{1}{V_\delta} \int_{D \cap B_\delta(x)} \omega^\delta(|y-x|) |y-x| \frac{\partial_t u(y) - \partial_t u(x)}{|y-x|} \cdot e_{y-x} dy \end{aligned} \quad (46)$$

and write

$$- \int_D \frac{1}{\delta^2} H^D(u)(x, t) \partial_t g(\theta(x, t; u)) dx = A(t) + B(t), \quad (47)$$

where

$$A(t) = - \int_D \frac{1}{\delta^2} H^D(u)(x, t) \partial_\theta g(\theta(x, t; u)) \frac{1}{V_\delta} \int_{D \cap B_\delta(x)} \omega^\delta(|y-x|) \partial_t u(y) \cdot e_{y-x} dy dx \quad (48)$$

and

$$B(t) = \int_D \frac{1}{\delta^2} H^D(u)(x, t) \partial_\theta g(\theta(x, t; u)) \frac{1}{V_\delta} \int_{D \cap B_\delta(x)} \omega^\delta(|y-x|) \partial_t u(x) \cdot e_{y-x} dy dx. \quad (49)$$

Next introduce the characteristic function of D denoted by $\chi_D(x)$ taking the value one inside D and zero outside, and together with the properties of $\omega^\delta(|y-x|)$, we rewrite $A(t)$ as

$$A(t) = - \int_{\mathbb{R}^3 \times \mathbb{R}^3} \chi_D(x) \chi_D(y) \omega^\delta(|y-x|) \frac{1}{\delta^2} H^D(u)(x, t) \partial_\theta g(\theta(x, t; u)) \frac{1}{V_\delta} \partial_t u(y) \cdot e_{y-x} dy dx; \quad (50)$$

we switch the order of integration and note $-e_{y-x} = e_{x-y}$ to obtain

$$A(t) = \int_D \frac{1}{V_\delta} \int_{D(x) \cap B_\delta(y)} \frac{\omega^\delta(|y-x|)}{\delta^2} H^D(u)(x, t) \partial_\theta g(\theta(x, t; u)) e_{x-y} dx \cdot \partial_t u(y) dy. \quad (51)$$

We can move $\partial_t u(x)$ outside the inner integral, regroup factors, and write $B(t)$ as

$$B(t) = \int_D \frac{1}{V_\delta} \int_{D \cap B_\delta(x)} \frac{\omega^\delta(|y-x|)}{\delta^2} H^D(u)(x, t) \partial_\theta g(\theta(x, t; u)) e_{y-x} dy \cdot \partial_t u(x) dx. \quad (52)$$

We rename the inner variable of integration y and the outer variable x in (51) and add equations (51) and (52) to get

$$A(t) + B(t) = \int_D \mathcal{L}^D(u)(x, t) \cdot \partial_t u(x, t) dx \quad (53)$$

and (44) is proved.

The steps used to prove (43) are similar to the proof of (44), so we provide only the key points of its derivation below. We expand $\partial_t f(\sqrt{|y-x|}S)$ to get

$$\begin{aligned} & \partial_t f(\sqrt{|y-x|}S(y, x, t; u)) \\ &= \partial_S f(\sqrt{|y-x|}S(y, x, t; u)) \frac{\partial_t u(y) - \partial_t u(x)}{|y-x|} \cdot e_{y-x}, \end{aligned} \quad (54)$$

and write

$$\begin{aligned} & - \frac{2}{V_\delta} \int_D \int_{D \cap B_\delta(x)} \frac{J^\delta(|y-x|)}{\delta} H^T(u)(y, x, t) \partial_t f(\sqrt{|y-x|}S(y, x, t; u)) dy dx \\ &= A(t) + B(t), \end{aligned} \quad (55)$$

where

$$\begin{aligned}
 A(t) &= \\
 &= - \int_D \frac{1}{V_\delta} \int_{D \cap B_\delta(x)} \frac{J^\delta(|y-x|)}{\delta|y-x|} H^T(u)(y, x, t) \partial_S \\
 &\quad f(\sqrt{|y-x|} S(y, x, t; u)) \partial_t u(y) \cdot e_{y-x} dy dx
 \end{aligned} \tag{56}$$

and

$$\begin{aligned}
 B(t) &= \\
 &= \int_D \frac{1}{V_\delta} \int_{D \cap B_\delta(x)} \frac{J^\delta(|y-x|)}{\delta|y-x|} H^T(u)(y, x, t) \partial_S \\
 &\quad f(\sqrt{|y-x|} S(y, x, t; u)) \partial_t u(x) \cdot e_{y-x} dy dx.
 \end{aligned} \tag{57}$$

We note that $S(y, x, t; u) = S(x, y, t; u)$ and $H^T(u)(y, x, t) = H^T(u)(x, y, t)$, and proceeding as in the proof of (44), we change the order of integration in (56) noting that $-e_{y-x} = e_{x-y}$ to get

$$\begin{aligned}
 A(t) &= \\
 &= \int_D \frac{1}{V_\delta} \int_{D \cap B_\delta(y)} \frac{J^\delta(|y-x|)}{\delta|y-x|} H^T(u)(x, y, t) \partial_S \\
 &\quad f(\sqrt{|y-x|} S(x, y, t; u)) e_{x-y} dx \cdot \partial_t u(y) dy.
 \end{aligned} \tag{58}$$

Taking $\partial_t u(x)$ outside the inner integral in (57) gives

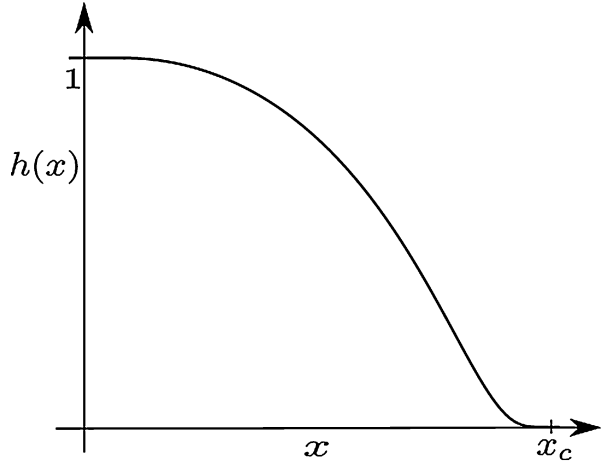
$$\begin{aligned}
 B(t) &= \\
 &= \int_D \frac{1}{V_\delta} \int_{D \cap B_\delta(x)} \frac{J^\delta(|y-x|)}{\delta|y-x|} H^T(u)(y, x, t) \partial_S \\
 &\quad f(\sqrt{|y-x|} S(y, x, t; u)) e_{y-x} dy \cdot \partial_t u(x) dx.
 \end{aligned} \tag{59}$$

We conclude noting that now

$$A(t) + B(t) = \int_D \mathcal{L}^T(u)(x, t) \cdot \partial_t u(x, t) dx, \tag{60}$$

and (43) is proved.

Fig. 5 Plot of $h(x)$ with $a = 2$



Explicit Damage Models, Cyclic Loading, and Strain to Failure

In this section, we provide concrete examples of the damage functions $H^T(u)(y, x, t)$ and $H^D(u)(x, t)$. We provide an example of cyclic loading and the associated degradation in the nonlocal force-strain law as well as the strain to failure curve for monotonically increasing strains. In this work, both damage functions H^T and H^D are given in terms of the function h . Here we give an example of $h(x) : \mathbb{R} \rightarrow \mathbb{R}^+$ as follows

$$h(x) = \begin{cases} \bar{h}(x/x_c), & \text{for } x \in (0, x_c), \\ 1, & \text{for } x \leq 0, \\ 0, & \text{for } x \geq x_c. \end{cases} \quad (61)$$

with $\bar{h} : [0, 1] \rightarrow \mathbb{R}^+$ is defined as

$$\bar{h}(x) = \exp\left[1 - \frac{1}{1 - (x/x_c)^a}\right] \quad (62)$$

where $a > 1$ is fixed. Clearly, $\bar{h}(0) = 1$, $\bar{h}(x_c) = 0$ (see Fig. 5).

For a given critical strain $S_c > 0$, we define the threshold function for tensile strain $j_S(x)$ as follows

$$j_S(x) := \begin{cases} \bar{j}(x/S_c), & \forall x \in [S_c, \infty), \\ 0, & \text{otherwise.} \end{cases} \quad (63)$$

where $\bar{j} : [1, \infty) \rightarrow \mathbb{R}^+$ is given by

Fig. 6 Plot of $j_S(x)$ with $a = 4, b = 5$ and $S_c = 2$

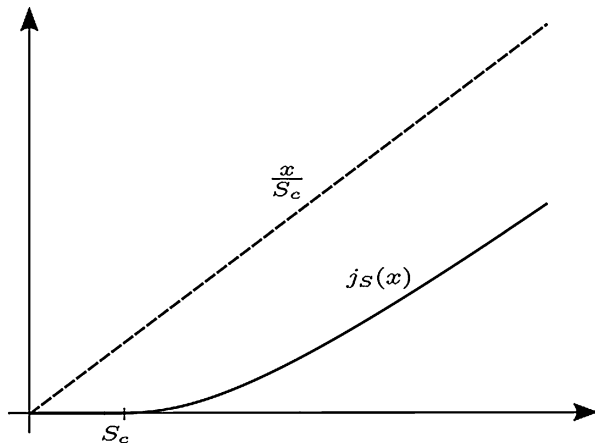
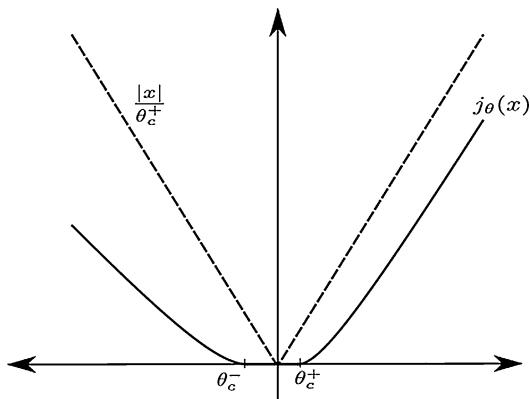


Fig. 7 Plot of $j_\theta(x)$ with $a = 4, b = 5, \theta_c^+ = 2,$ and $\theta_c^- = 3$



$$\bar{j}(x) = \frac{(x-1)^a}{1+x^b} \quad (64)$$

with $a > 1$ and $b \geq a - 1$ fixed. Note that $j_S(1) = 0$. Here the condition $b \geq a - 1$ insures the existence of a constant $\gamma > 0$ for which

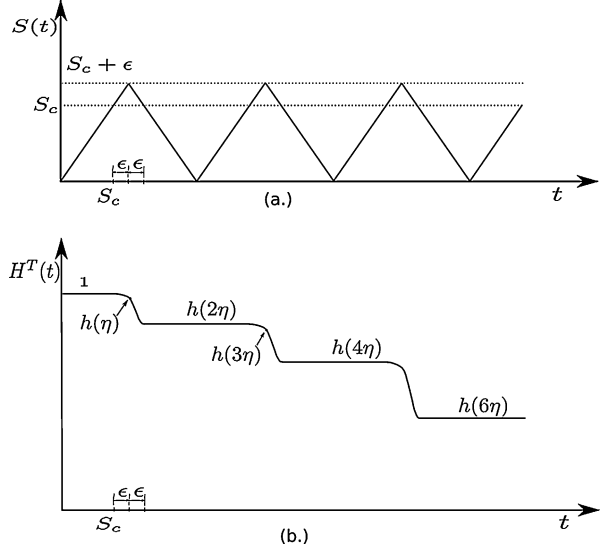
$$j_S(x) \leq \gamma|x|, \quad \forall x \in \mathbb{R} \quad (65)$$

(see Fig. 6).

For a given critical hydrostatic strains $\theta_c^- < 0 < \theta_c^+$, we define the threshold function $j_\theta(x)$ as

$$j_\theta(x) := \begin{cases} \bar{j}(x/\theta_c^+), & \forall x \in [\theta_c^+, \infty), \\ \bar{j}(-x/\theta_c^-), & \forall x \in (-\infty, -\theta_c^-], \\ 0, & \text{otherwise,} \end{cases} \quad (66)$$

Fig. 8 (a) Strain profile. (b) Damage function plot corresponding to strain profile



where $\bar{j}(x)$ is defined by (64), and we plot j_θ in Fig. 7. We summarize noting that an explicit form for $H^T(u)(y, x, t)$ is obtained by using (61) and (63) in (8) and an explicit form for $H^D(u)(x, t)$ is obtained by using (61) and (66) in (9).

We first provide an example of cyclic damage incurred by a periodically varying tensile strain. Let x, y be two fixed material points with $|y - x| < \delta$, and let $S(y, x, t; u) = S(t)$ correspond to a temporally periodic strain (see Fig. 8a). Here $S(t)$ periodically takes excursions above the critical strain S_c . During the first period, we have

$$S(t) = \begin{cases} t, & \forall t \in [0, S_c + \epsilon], \\ 2(S_c + \epsilon) - t & \forall t \in (S_c + \epsilon, 2(S_c + \epsilon)] \end{cases}$$

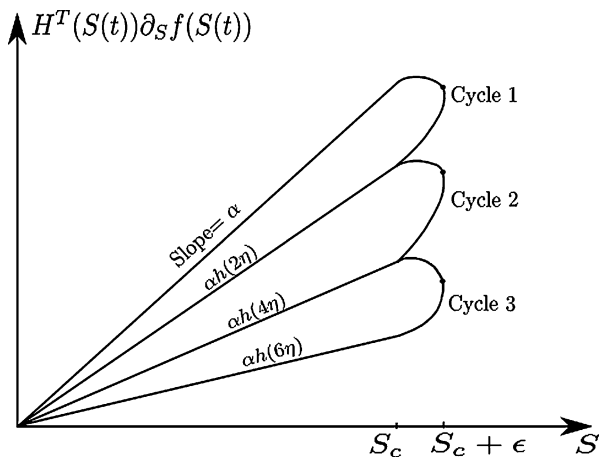
and $S(t)$ is extended to \mathbb{R}^+ by periodicity (see Fig. 8a). For this damage model, we let η be the area under the curve $j_S(x)$ from $x = S_c$ to $x = S_c + \epsilon$. It is given by

$$\eta = \int_{S_c}^{S_c + \epsilon} j_S(x) dx = \int_{S_c}^{S_c + \epsilon} j_S(S(t)) dt.$$

From symmetry, the area under the curve $j_S(x)$ under unloading from $S_c + \epsilon$ to S_c is also η . The corresponding damage function $H^T(u)(y, x, t)$ is plotted in Fig. 8b.

In Fig. 9, we plot the strain-force relation where S is the abscissa and the tensile force given by $H^T(u)(y, x, t) \partial_S f(\sqrt{|y - x|} S(y, x, t; u))$ is the ordinate. Here the damage factor $H^T(u)(y, x, t)$ drops in value with each cycle of strain loading. After each cycle, the slope (elasticity) in the linear and recoverable part of the force-strain curve decreases due to damage. The force needed to soften the material is the

Fig. 9 Cyclic strain vs Force plot. The initial stiffness is α . Hysteresis is evident in this model



strength, and it is clear from the model that the strength decreases after each cycle due to damage.

Application of this rigorously established model to fatigue is a topic of future research but beyond the scope of this article. We note that fatigue models based on peridynamic bond softening are introduced in Oterkus (2010) and with fatigue crack nucleation in the context of the Paris law in Silling and Askari (2014).

The next example is strain to failure for a monotonically increasing strain. Here we let

$S(y, x, t; u) = S(t) = t$ and plot the corresponding force-strain curve in Fig. 10. We see that the force-strain relation is initially linear until the strain exceeds S_c ; the force then reaches its maximum and subsequently softens to failure. At $S^* \approx 0.55025$, we have $\int_0^{S^*} j_S(t) dt = x_c$ and $H^T = 0$. Here we take $\alpha = 1$.

Numerical Results

In this section, we present numerical results. Explicit expressions of the functions described in the previous section are used in simulating the problem. The damage function h is defined similar to Eq. 61 with exponents $a = 1.01$ and $x_c = 0.2$. The function j_S is given by Eq. 63 with $a = 5, b = 5, S_c = 0.01$. The function j_θ is given by Eq. 66 with $a = 4, b = 5, \theta_c^+ = 0.3, \theta_c^- = 0.4$. Nonlinear potential function f is given by $f(r) = \alpha r^2$ for $r < r_1$ and $f(r) = r$ for $r > r_2$. We let $\alpha = 10$ and let $r_1 = r_2 = 0.05$. Similarly, the nonlinear potential function g is given by $g(r) = \beta r^2$ for $r < r_1^*$ and $g(r) = r$ for $r > r_2^*$. We let $\beta = 1$ and let $r_1^* = r_2^* = 0.05$. The influence function is given by $J^\delta(|y - x|) = \omega^\delta(|y - x|) = 1 - \frac{|y-x|}{\delta}$ for $0 \leq |y - x| \leq \delta$ and $J^\delta(|y - x|) = \omega^\delta(|y - x|) = 0$ otherwise. We consider θ_c^+ and θ_c^- sufficiently high so that we only see damage due to tensile forces and not hydrostatic forces.

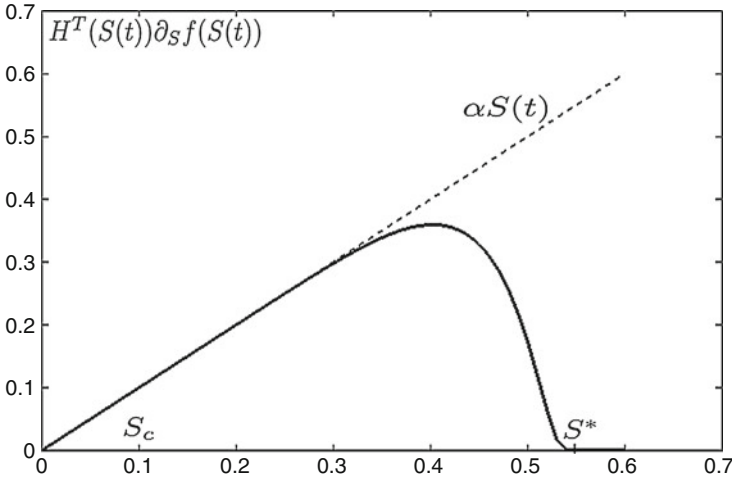


Fig. 10 Strain vs force plot where $S(t) = t$. $H^T(S(t))$ begins to drop at $S_c = 0.1$ and $S^* \approx 0.55025$

In both numerical problems, we consider the material domain $D = [0, 1]^2$. We also keep the initial condition fixed to $u_0 = 0$ and $v_0 = 0$. Further, we apply no body force, i.e., $b = 0$. However we will consider boundary loading that is periodic in time. Let $x = (x_1, x_2)$ where x_1 corresponds to the component along horizontal axis and x_2 corresponds to the component along vertical axis.

Periodic Loading

We apply boundary condition $u = 0$ on edge $x_1 = 0$, $x_1 = 1$, and $x_2 = 0$. We consider function \bar{u} of form

$$\bar{u}(t) = \begin{cases} \alpha_{bc} t, & \forall t \in [0, T_{bc}], \\ \alpha_{bc} T_{bc} - t & \forall t \in (T_{bc}, 2T_{bc}] \end{cases} \quad (67)$$

and periodically extend the function for any time t . For point x on edge $x_2 = 1$, we apply $u(t, x) = (u_1(t, x), u_2(t, x)) = (0, \bar{u}(t))$. We consider $\alpha_{bc} = 0.01$ and $T_{bc} = 0.216$.

To numerically approximate the evolution equation, we discretize the domain D uniformly with mesh size $h = \delta/5$, where $\delta = 0.15$ in this problem. For time discretization, we consider the velocity Verlet scheme for second order in time differential equation and a midpoint quadrature for the spatial discretization. Final time is $T = 1.2$ and size of time step is $\Delta t = 10^{-5}$.

To obtain the hysteresis plot, we chose bonds as shown in Fig. 11. We track the bond strain $S(y, x, t; u)$ and other relevant quantities. While we track all the bonds

Fig. 11 Discretization of material domain $D = [0, 1]^2$. During simulation bond between red and black material point is tracked to obtain the strain vs stress profile and other information

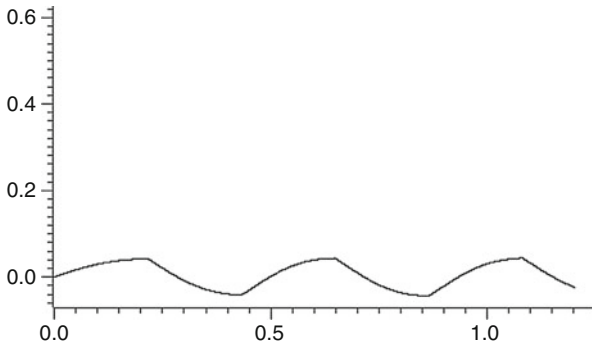
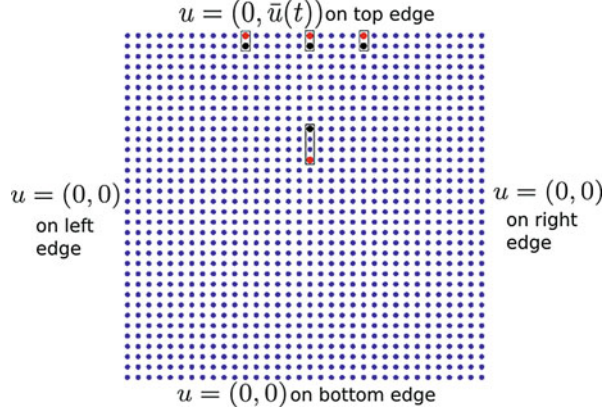


Fig. 12 Time vs Strain $S(y, x, t; u)$ plot

shown in Fig. 11, we only provide plots for the bond which is near to middle top edge. For the bonds in either left and right of the bond at middle top edge, the response is the same. For the bond inside the material, the strains are never greater than S_c , and therefore it experiences no damage.

Figures 12 and 13 show the strain of the bond and damage H^T of the bond as function of time. It is quite similar to the plots shown in Figs. 8 and 9. In Fig. 14, we show the strain vs force plot. Red line shows response of bond when damage function is taken to be unity. We further note that the damage is defined for positive strains above critical strain.

Shear Loading

We apply $u = 0$ on bottom edge and keep left and right edge free. On top, we apply $u(t, x) = (u_1(t, x), u_2(t, x)) = (\gamma t x_2, 0)$. We chose $\gamma = 0.0001$ and simulate the problem up to time $T = 750$. Time step is $\Delta t = 10^{-5}$.

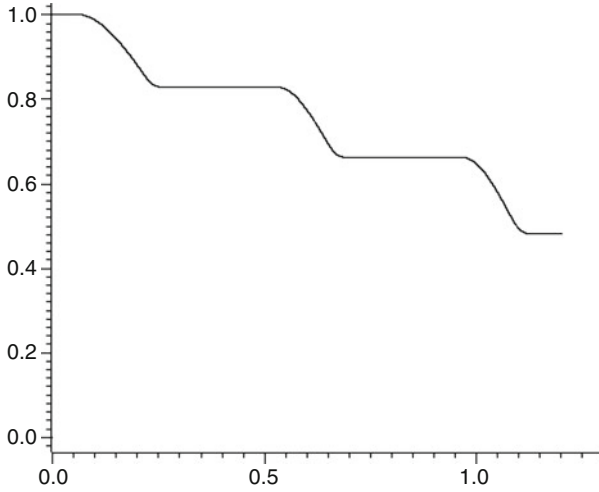


Fig. 13 Time vs Damage function $H^T((u)(y, x, t))$ plot

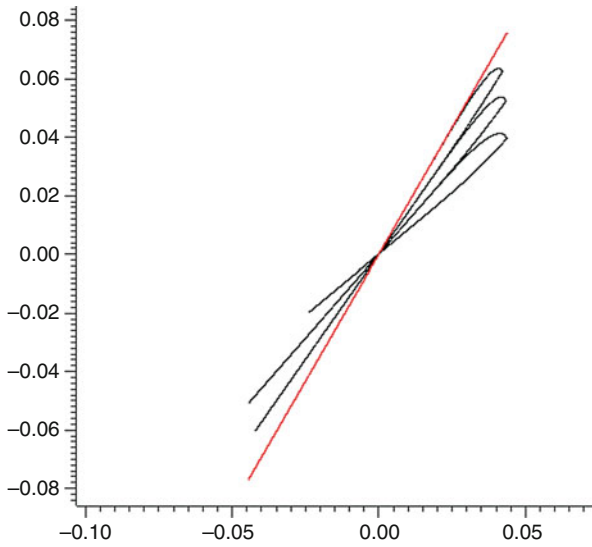
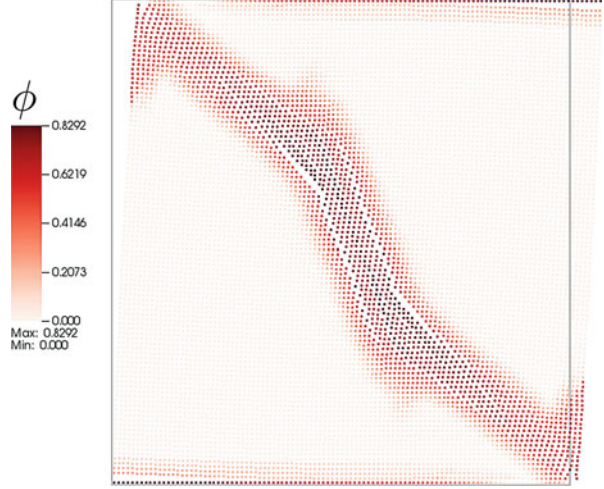


Fig. 14 Strain $S(y, x, t; u)$ vs Stress $H^T((u)(y, x, t))\partial_S f(\sqrt{|y-x|}S(y, x, t; u))$ plot for the bond near middle top edge. Red color corresponds to $\partial_S f(\sqrt{|y-x|}S(y, x, t; u))$

Fig. 15 Each point in figure shows the discretized mesh node. Strength of color shows the damage ϕ experienced by the mesh node. Box shows reference material domain $[0, 1]^2$



We choose the size of horizon to be $\delta = 0.05$ and mesh size $h = \delta/5$. As noted in the beginning of the section that we choose hydrostatic parameters large enough such that the damage is only due to the tensile interaction between material points. For tensile interaction, the extent of damage experienced by a material is defined as

$$\phi(t, x; u) = 1 - \frac{\int_{D \cap B_\delta(x)} H^T(u)(y, x, t) dy}{\int_{D \cap B_\delta(x)} dy}. \quad (68)$$

Clearly, if all bonds in a horizon of material point x suffer no damage, then ϕ will be 0. As the damage of bonds increases, ϕ also increases. In Fig. 15, we show ϕ at final time $t = 750$. As we can see, the damage is along the diagonal of square.

Linear Elastic Operators in the Small Horizon Limit

In this section, we consider smooth evolutions u in space and show that away from damage set, the operators $\mathcal{L}^T + \mathcal{L}^D$ acting on u converge to the operator of linear elasticity in the limit of vanishing nonlocality. We denote the damage set by \tilde{D} and consider any open undamaged set D' interior to D with its boundary a finite distance away from the boundary of D and the damage set \tilde{D} . In what follows, we suppose that the nonlocal horizon δ is smaller than the distance separating the boundary of D' from the boundaries of D and \tilde{D} .

Theorem 3. *Convergence to linear elastic operators. Suppose that $u(x, t) \in C^2([0, T_0], C^3(D, \mathbb{R}^3))$ and no damage, i.e., $H^T(y, x, t) = 1$ and $H^D(x, t) = 1$, for every $x \in D' \subset D \setminus \tilde{D}$, then there is a constant $C > 0$ independent of nonlocal horizon δ such that for every (x, t) in $D' \times [0, T_0]$, one has*

$$|\mathcal{L}^T(u(t)) + \mathcal{L}^D(u(t)) - \nabla \cdot \mathbb{C} \mathcal{E}(u(t))| < C \delta, \quad (69)$$

where the the elastic strain is $\mathcal{E}(u) = (\nabla u + (\nabla u)^T)/2$ and the elastic tensor is isotropic and given by

$$\mathbb{C}_{ijkl} = 2\mu \left(\frac{\delta_{ik}\delta_{jl} + \delta_{il}\delta_{jk}}{2} \right) + \lambda \delta_{ij}\delta_{kl}, \quad (70)$$

with shear modulus μ and Lamé coefficient λ given by

$$\mu = \frac{f''(0)}{10} \int_0^1 r^3 J(r) dr \text{ and } \lambda = g''(0) \left(\int_0^1 r^3 J(r) dr \right)^2 + \frac{f''(0)}{10} \int_0^1 r^3 J(r) dr. \quad (71)$$

The numbers $f''(0) = \alpha$ and $g''(0) = \beta$ can be chosen independently and can be any pair of real numbers such that \mathbb{C} is positive definite.

Proof. We start by showing

$$|\mathcal{L}^T(u(t)) - \frac{f''(0)}{2\omega_3} \int_{B_1(0)} e|\xi|J(|\xi|)e_i e_j e_k d\xi \partial_{jk}^2 u_i(x)| < C \delta, \quad (72)$$

where $\omega_3 = 4\pi/3$ and $e = e_{y-x}$ are unit vectors on the sphere; here repeated indices indicate summation. To see this, recall the formula for $\mathcal{L}^T(u)$ and write $\partial_S f(\sqrt{|y-x|}S) = f'(\sqrt{|y-x|}S)\sqrt{|y-x|}$. Now Taylor expand $f'(\sqrt{|y-x|}S)$ in $\sqrt{|y-x|}S$, and Taylor expand $u(y)$ about x , denoting e_{y-x} by e to find that all odd terms in e integrate to zero and

$$\begin{aligned} |\mathcal{L}^T(u(t))_l - \frac{2}{V_\delta} \int_{B_\delta(x)} \frac{J^\delta(|y-x|)}{\delta|y-x|} \frac{f''(0)}{4} |y-x|^2 \partial_{jk}^2 u_i(x) e_i e_j e_k e_l, dy| \\ < C \delta, \quad l = 1, 2, 3. \end{aligned} \quad (73)$$

On changing variables $\xi = (y-x)/\delta$, we recover (72). Now we show

$$\begin{aligned} |\mathcal{L}^D(u(t))_k - \frac{1}{\omega_3} \int_{B_1(0)} |\xi|\omega(|\xi|)e_i e_j d\xi \frac{g''(0)}{\omega_3} \int_{B_1(0)} |\xi|\omega(|\xi|)e_k e_l d\xi \partial_{ij}^2 u_i(x)| \\ < C \delta, \quad k = 1, 2, 3. \end{aligned} \quad (74)$$

We note for $x \in D'$ that $D \cap B_\delta(x) = B_\delta(x)$ and the integrand in the second term of (6) is odd and the integral vanishes. For the first term in (6), we Taylor expand $\partial_\theta g(\theta)$ about $\theta = 0$ and Taylor expand $u(z)$ about y inside $\theta(y, t)$ noting that terms odd in $e = e_{z-y}$ integrate to zero to get

$$|\partial_\theta g(\theta(y, t)) - g''(0) \frac{1}{V_\delta} \int_{B_\delta(y)} \omega^\delta(|z-y|) |z-y| \partial_j u_i(y) e_i e_j dz| < C \delta^3. \quad (75)$$

Now substitution for the approximation to $\partial_\theta g(\theta(y, t))$ in the definition of \mathcal{L}^D gives

$$\begin{aligned} & |\mathcal{L}^D(u) \\ & - \frac{1}{V_\delta} \int_{B_\delta(x)} \frac{\omega^\delta(|y-x|)}{\delta^2} e_{y-x} \frac{1}{V_\delta} \int_{B_\delta(y)} \omega^\delta(|z-y|) |z-y| g''(0) \partial_j u_i(y) e_i e_j dz dy| < C \delta. \end{aligned} \quad (76)$$

We Taylor expand $\partial_j u_i(y)$ about x , note that odd terms involving tensor products of e_{y-x} vanish when integrated with respect to y in $B_\delta(x)$, and we obtain (74).

We now calculate as in (Lipton 2016, equation (6.64)) to find that

$$\begin{aligned} & \frac{f''(0)}{2\omega_3} \int_{B_1(0)} |\xi| J(|\xi|) e_i e_j e_k e_l d\xi \partial_{jk}^2 u_i(x) \\ & = \left(2\mu_1 \left(\frac{\delta_{ik}\delta_{jl} + \delta_{il}\delta_{jk}}{2} \right) + \lambda_1 \delta_{ij}\delta_{kl} \right) \partial_{jk}^2 u_i(x), \end{aligned} \quad (77)$$

where

$$\mu_1 = \lambda_1 = \frac{f''(0)}{10} \int_0^1 r^3 J(r) dr. \quad (78)$$

Next observe that a straight forward calculation gives

$$\frac{1}{\omega_3} \int_{B_1(0)} |\xi| \omega(|\xi|) e_i e_j d\xi = \delta_{ij} \int_0^1 r^3 \omega(r) dr, \quad (79)$$

and we deduce that

$$\begin{aligned} & \frac{1}{\omega_3} \int_{B_1(0)} |\xi| \omega(|\xi|) e_i e_j d\xi \frac{g''(0)}{\omega_3} \int_{B_1(0)} |\xi| \omega(|\xi|) e_k e_l d\xi \partial_{ij}^2 u_i(x) \\ & = g''(0) \left(\int_0^1 r^3 \omega(r) dr \right)^2 \delta_{ij}\delta_{kl} \partial_{ij}^2 u_i(x). \end{aligned} \quad (80)$$

Theorem 3 follows on adding (77) and (80) □

Conclusions

We have introduced a simple nonlocal model for free damage propagation in solids. In this model, there is only one equation, and it describes the dynamics of the displacement using Newton's law $F = ma$. The damage is a consequence of

displacement history and diminishes the force-strain law as damage accumulates. The modeling allows for both cyclic damage or damage due to abrupt loading. The damage is irreversible, and the damage set grows with time. The dissipation energy due to damage together with the kinetic and potential energy satisfies energy balance at every instant of the evolution. Future work will address the question of localization of damage using this model. We believe that if the loading is such that large monotonically increasing strains are generated, then damage localization based on material softening and inertia could be anticipated.

In this treatment, we have considered dynamic problems only. For this case, we have shown uniqueness for the model. The analysis of this model in the absence of inertial forces leads to the quasi-static case where the effects of inertia are absent but memory of the load history is still present. Future work aims to explore this model for this case and understand regimes of body force specimen geometry and boundary loads for which there is loss of uniqueness and associated instability. Such nonuniqueness is well known for quasi-static gradient damage models (Pham and Marigo, 2013).

Acknowledgements This material is based upon the work supported by the U S Army Research Laboratory and the U S Army Research Office under contract/grant number W911NF1610456.

References

- A. Agwai, I. Guven, E. Madenci, Predicting crack propagation with peridynamics: a comparative study. *Int. J. Fract.* **171**, 65–78 (2011)
- F. Bobaru, W. Hu, The meaning, selection, and use of the peridynamic horizon and its relation to crack branching in brittle materials. *Int. J. Fract.* **176**, 215–222 (2012)
- F. Bobaru, J.T. Foster, P.H. Geubelle, S.A. Silling, *Handbook of Peridynamic Modeling* (CRC Press, BOCA Ratone, 2016)
- K. Dayal, K. Bhattacharya, Kinetics of phase transformations in the peridynamic formulation of continuum mechanics. *J. Mech. Phys. Solids* **54**, 1811–1842 (2006)
- Q. Du, Y. Tao, X. Tian, A peridynamic model of fracture mechanics with bond-breaking. *J. Elast.* (2017). <https://doi.org/10.1007/s10659-017-9661-2>
- E. Emmrich, D. Phust, A short note on modeling damage in peridynamics. *J. Elast.* **123**, 245–252 (2016)
- E. Emmrich, O. Weckner, On the well-posedness of the linear peridynamic model and its convergence towards the Navier equation of linear elasticity. *Commun. Math. Sci.* **5**, 851–864 (2007)
- J.T. Foster, S.A. Silling, W. Chen, An energy based failure criterion for use with peridynamic states. *Int. J. Multiscale Comput. Eng.* **9**, 675–688 (2011)
- W. Gerstle, N. Sau, S. Silling, Peridynamic modeling of concrete structures. *Nuclear Eng. Des.* **237**, 1250–1258 (2007)
- Y.D. Ha, F. Bobaru, Studies of dynamic crack propagation and crack branching with peridynamics. *Int. J. Fract.* **162**, 229–244 (2010)
- P. K. Jha, R. Lipton, Numerical analysis of peridynamic models in Hölder space, arXiv preprint arXiv:1701.02818 (2017)
- R. Lipton, Dynamic brittle fracture as a small horizon limit of peridynamics. *J. Elast.* **117**, 21–50 (2014)
- R. Lipton, Cohesive dynamics and brittle fracture. *J. Elast.* **124**(2), 143–191 (2016)

- R. Lipton, S. Silling, R. Lehoucq, Complex fracture nucleation and evolution with nonlocal elastodynamics. arXiv preprint arXiv:1602.00247 (2016)
- R. Lipton, E. Said, P.K. Jha, Free damage propagation with memory. *J. Elast.* To appear in *J. Elasticity* (2018)
- T. Mengesha, Q. Du, Nonlocal constrained value problems for a linear peridynamic Navier equation. *J. Elast.* **116**, 27–51 (2014)
- E. Oterkus, I. Guven, E. Madenci, Fatigue failure model with peridynamic theory, in *IEEE Intersociety Conference on Thermal and Thermomechanical Phenomena in Electronic Systems (ITherm)*, Las Vegas, June 2010, pp. 1–6
- K. Pham, J.J. Marigo, From the onset of damage to rupture: construction of responses with damage localization for a general class of gradient damage models. *Contin. Mech. Thermodyn.* **25**, 147–171 (2013)
- S.A. Silling, Reformulation of elasticity theory for discontinuities and long-range forces. *J. Mech. Phys. Solids* **48**, 175–209 (2000)
- S.A. Silling, E. Askari, A meshfree method based on the peridynamic model of solid mechanics. *Comput. Struct.* **83**, 1526–1535 (2005)
- S.A. Silling, E. Askari, Peridynamic model for fatigue cracking. Sandia Report, SAND2014-18590, 2014
- S.A. Silling, F. Bobaru, Peridynamic modeling of membranes and fibers. *Int. J. Nonlinear Mech.* **40**, 395–409 (2005)
- S.A. Silling, M. Epton, O. Weckner, J. Xu, E. Askari, Peridynamic states and constitutive modeling. *J. Elast.* **88**, 151–184 (2007)
- S.A. Silling, R.B. Lehoucq, Convergence of peridynamics to classical elasticity theory. *J. Elast.* **93**, 13–37 (2008)
- S. Silling, O. Weckner, E. Askari, F. Bobaru, Crack nucleation in a peridynamic solid. *Int. J. Fract.* **162**, 219–227 (2010)
- O. Weckner, R. Abeyaratne, The effect of long-range forces on the dynamics of a bar. *J. Mech. Phys. Solids* **53**, 705–728 (2005)
- O. Weckner, E. Emmrich, Numerical simulation of the dynamics of a nonlocal, inhomogeneous, infinite bar. *J. Comput. Appl. Mech.* **6**, 311–319 (2005)